Finding the low-energy structures of Si[001] symmetric tilted grain boundaries with a genetic algorithm

Jian Zhang, Cai-Zhuang Wang, and Kai-Ming Ho
U.S. Department of Energy, Ames Laboratory, Ames, Iowa 50011, USA
and Department of Physics, Iowa State University, Ames, Iowa 50011, USA
(Received 13 April 2009; published 4 November 2009)

We developed a global structure optimization method, genetic algorithm, for a fast and efficient prediction of grain-boundary structures. Using this method we predicted the most stable structures and a number of low-energy metastable structures for Si[001] symmetric tilted grain boundaries with various tilted angles. We show that most of the grain-boundary structures can be described by the structural unit model with the units being the dislocation cores and perfect-crystal fragments. The energies of the grain-boundary structures obtained from the genetic algorithm optimization are evaluated by tight-binding calculations using the environment-dependent Si tight-binding potential developed previously and found to be in very good agreement with the first-principles calculation results.

DOI: 10.1103/PhysRevB.80.174102 PACS number(s): 78.67.Lt, 73.22.−f, 73.21.Hb

I. INTRODUCTION

Grain boundaries (GB) play an important role in microstructure stability, mechanical behavior, and transport properties of many polycrystalline materials. Grain boundaries are also considered to be the major defects affecting the performance of many microelectronic materials and devices, such as micromechanical materials, nanocrystalline materials, and solar-energy-application devices.[1–4] Therefore understanding the structures of grain boundaries at the atomic level is highly desirable. However, structural complexity of grain boundaries makes both experimental and theoretical studies difficult. Although the experimental tools such as high-resolution transmission electron microscopy (HRTEM) are widely used in studying grain boundaries in materials, the experimental resolution necessary to examine the detailed atomic structure of grain boundary is still difficult to achieve. On the other hand, many possible structures for a given grain boundary also makes theoretical study complicated.[4–10] The relatively large system size (hundreds to thousands atoms) makes first-principles calculations very costly. Meanwhile, many classical potentials, which are fast and useful for calculating system with large size, need to be checked for their accuracy.[4–10]

The atomic structures of grain boundaries in Si have received lots of interest both experimentally and theoretically.[4–10] Ball and stick modeling is first used to deduce plausible reconstructions based on the hypothesis that the coordination in grain-boundary structures preserve that of crystals as far as possible.[1,2] Further modeling using molecular dynamics, Monte Carlo annealing is also used to explore possible GB structures.[10–12] Among those studies Si[001] symmetric tilted grain boundaries have attracted the most interest. The energies of symmetrical tilted GB in Si have been characterized using lots of calculation methods including first-principles density-functional theory (DFT) calculations, semiempirical tight-binding (TB) methods, analytical bond-order potential and other classical potentials.[4–10]

In this paper we will use an efficient global optimization method, genetic algorithm (GA) to generate the structure of grain boundary. Genetic algorithm is an optimization strategy inspired by the Darwinian evolution process. The GA operation is analogous to the process of natural selection of the fittest offsprings. At the end of each GA run, the fittest structures are remaining in the GA pool. GA has already enjoyed huge successes in determining the structures of various dimensions including atomic clusters, crystal structures, nanowires, and surface structures.[13–18]

There are two clear advantages of genetic algorithm over the other methods: (1) genetic algorithm has an effective way of overcoming energy barriers by its mating algorithm. When designed properly, it can explore extensively into the whole energy landscape without trapping into the local minimum for too long. On the other hand, other methods such as molecular dynamics or Monte Carlo approach are not easy to move the system out of the local minimum. Therefore the efficiency in GA can be much better than other methods especially when the overall energy landscape has many local minimums and the energy barriers between these minimums are high. (2) Usually genetic algorithm requires little information on the initial structure. It does not make assumptions on the shape or topology of the energy landscape. The first generation of structures in GA are almost always produced randomly without starting from certain initial structures. While in other methods reasonably good starting structures are often needed in order to make transitions to the desired structures.

This paper is arranged as follows. In Sec. II, the GA method used in our grain-boundary-structure optimization will be discussed in details. The grain-boundary structures obtained from our GA search are presented in Sec. III. The energies of the grain boundary are further discussed in Sec. IV followed by the summary in Sec. V.

II. GENETIC ALGORITHM FOR GRAIN-BOUNDARY-STRUCTURE OPTIMIZATION

Symmetrical tilted Si[001] GB can be constructed by rotating the two Si grains in the opposite direction by the same angle around the (001) rotation axis and then matching the

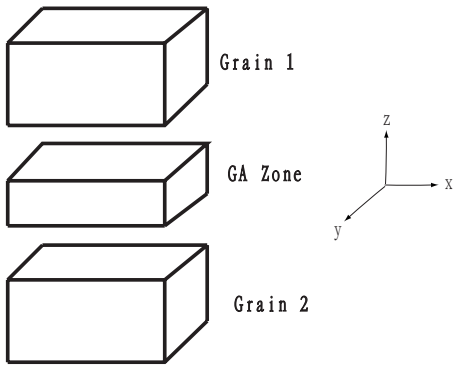

FIG. 1. The computation cell for the GA search. x and y directions are periodic while z direction is terminated at free surfaces. The interface area between the two grains are called the GA zone.

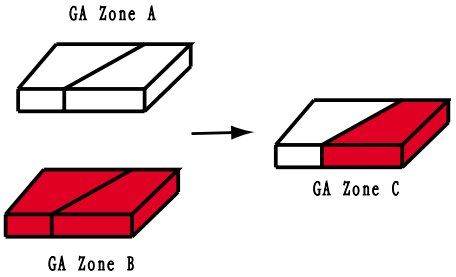

FIG. 2. (Color online) The mating operation $\mathcal{O}:(\mathrm{A},\mathrm{B}\rightarrow\mathrm{C})$ From the two candidate structures A and B, which are separated by the same arbitrary plane oriented perpendicular to the surface. A new slab C is created by combining the part A that lies to the left of the cutting plane and the part of slab B which is laying to the left of the plane. C is placed between the two grains and the resulting structure is totally relaxed.

two grains together.[12] Thus in the direction of the boundary plane the GB will show periodic structures. We model the GB using a simulation block with periodic conditions in the directions parallel to the boundary plane (x and y). In the perpendicular direction z, the grains are terminated at free surfaces. The geometry and dimensions of the computational cells are shown in Fig. 1. Atomic positions in the cell are generated from geometrical coincident site lattice construction. In this geometry, the rigid-body translations are free to occur if they lead to more energetically favorable structures. The thickness of the grains in the z direction is chosen to be large enough to exclude interactions between the GB and surfaces. This is ensured by performing the calculations with different thicknesses and verify that the results are nearly the same. In this paper the thickness is chosen to be ten times of the period in the x direction.

A special designed genetic algorithm is used to produce the structures of grain boundaries. The atomic structure of grain boundaries can be seen as a reconstruction of the interface atoms between two grains. We first define a GA zone by choosing a slab at the interface between the two grains, as shown in Fig. 1. The GA operations will be run on the atoms inside the GA zone while atoms outside the GA zone are allowed to relax to a local minimum of the potential energy after each GA operation.

The optimization procedure developed here is based on the idea of evolutionary approach in which the number of a generation (pool of models for the interface) is generated with the goal of producing the best specimens, i.e., lowest-energy reconstructions. We can divide the algorithm in the following steps.

The first step is initial pool construction, which we call "generation zero." In the beginning we will have a pool of p different structures obtained by randomizing the positions of the atoms inside the GA zone and by subsequently relaxing the simulation cell through molecular static relaxation.

The second step is mating, which is the evolution from one generation to the next one. We can generate an offspring structure from two randomly picked structures in the pool of current generation through a mating operation: $\mathcal{O}:(\mathrm{A},\mathrm{B}\rightarrow\mathrm{C})$. As in Fig. 2 two parent structures A and B are randomly selected from the pool and the two GA zones are separated and sectioned by an arbitrary plane perpendicular to the surface of the cells. The new GA zone is created by combining the part of A that lies to the left of the cutting plane and the part of B lying to the right of that plane. Then the new GA zone is combined with the rest parts (either from A or B) to form a new child structure C. Structure C is then further relaxed to the nearest local minimum with conjugate gradient minimization. Two versions of the genetic algorithm are developed. In the first version the number of atoms inside the GA zone is kept constant by automatically rejecting the child structures that have different number of atoms from their parents in the GA zone. In the second one the restriction is not enforced thus it is possible to have a different number of atoms in the child than its parent. Here we choose the second version as it allows us to do a wider range of search over more different structures. In each generation, a number of m mating operations are performed.

The third step is updating the pool. From mating step above we have m children structures. They are relaxed and considered for the possible inclusion in the pool based on their grain-boundary energy. If there exist at least one candidate in the pool that has a higher grain-boundary energy than that of the child considered then the child structure is included in the pool. Upon inclusion of the child, the structure with the highest grain-boundary energy is discarded in order to preserve the total population p. To avoid crowding the pool with identical metastable configurations, we retain a new structure only if its energy differs by more than δ when compared to the energy of any of the current member p of the pool. We also consider a criterion based on atomic displacements to account for the (theoretically possible) situation in which two structures have equal energy but different topologies: two structures are considered structurally different if the relative displacement of at least one pair of corresponding atoms is greater than ϵ. Relevant values for the parameters of the genetic algorithms are $p=30$, $m=15$, $d=5A$, $\delta=10^{-5}$, and $\epsilon=0.2A$

The fourth step is to repeat the mating process in a new generation and update the pool after m mating operations are done. We can keep repeating for hundreds to thousands of generations until the desired structures are found in the pool.

III. STRUCTURES GENERATED BY THE GENETIC ALGORITHM

A symmetrical Si[001] tilt grain boundary can be described as a GB with median plane (110) or (100) and a rotation angle with the range from 0° to 90°.[9] We searched for the structures of Si GB's at 18 disorientation angles with GA using the classical Stillinger-Weber potential. In each GA run, after a number of generations, final structures can be obtained from the GA pools. In each pool we can find the ground-state structure, which is the structure with the lowest energy calculated using the Stillinger-Weber potential together with many higher-energy metastable structures. These lowest-energy structures are in agreement with previous theoretical and experimental results while they are produced by GA with much higher efficiency. In Figs. 4–7 we show the GB structures of four different orientation angles from 0° to 90°, respectively. In these figures, we show not only the lowest-energy structures but also some lower-energy metastable structures. After a careful look at the results we can see that the structural-unit model is generally a good description of the structures we have found. The structural-unit model describes GB's in terms of structural units (SU's) consisting of either the perfect-crystal structure or dislocation cores with the associated Burgers vectors.[10,11] The majority of Si[001] symmetrical tilted GB's in the entire range of disorientation can be constructed from three characteristic structural units as shown in Fig. 3: unit A, a pure edge-dislocation core, with a burgers vector $b=\frac{1}{2}a_0[110]$, where a_0 is the lattice constant of the perfect crystal; unit B, the core of a 45° mixed dislocation, with burgers vector inclined at 45° to the rotation axis. This mixed dislocation core has a screw component, which is parallel to the rotation axis; unit C, the unit of a perfect crystal. Also we can see that there are generally two basic ways how those structural units are connected to form the grain boundary: the straight way or the zigzag way. The sequence of the structural units arranged and the way they are connected will have an impact on the GB energies they have, which we will illustrate in the following examples.

In Fig. 4 we show a typical example of the small-angle grain boundary with tilted angle 16.26°. For ground-state structures with the small angles the grain-boundary structures can often be seen as rows of parallel pure edge dislocations (unit A), which is a pentagonal-triangular pattern shared with a same edge, separated by a series of good crystal units (unit C). In this case the structure Fig. 4(a) has two dislocation core structures separated by five crystal structure units between them, which gives a *CCCCCACCCCCA* arrangement in the GB area. This structure also has a mirrorlike symmetry across the boundary plane. The structures shown in Figs. 4(b)–4(d) are some of the higher energy structures in the pool. Among b,c,d only structure Fig. 4(c) preserve the mirrorlike symmetry across the GB plane. Structure Fig. 4(c) has the same set of units as structure Fig. 4(a). However it has a different unit arrangement as *CCCACCCCCCCA*, which results in higher GB energy. Structure Fig. 4(b) has similar units arrangement but the dislocation cores are shifted apart in the (110) direction, which causes a higher energy. Structure Fig. 4(d) can be seen as formed by the addition of extra dislocations introduced to the Fig. 4(a) structure, which will also raise the GB energy. Besides those four structures, there are also numerous new structures in this rotation angle in the GA pool, which shows

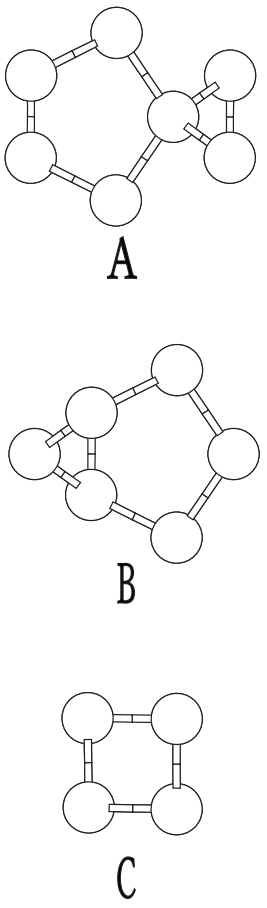

FIG. 3. The SU's for the Si[001] symmetrical tilted grain boundaries. Three types of units are available: A is a core of pure edge dislocation, B is a mixed core dislocation with screw component, and C is the unit of a perfect-crystal structure.

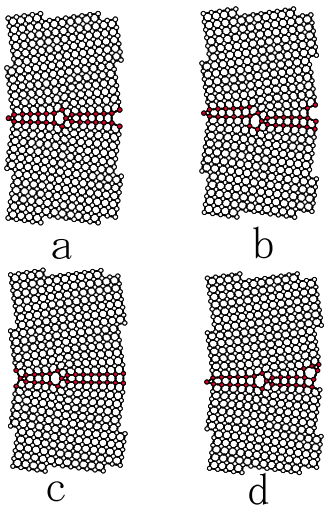

FIG. 4. (Color online) Atomic structures of $\Sigma=25$ Si[001](340) GB with rotation angle $\theta=16.26°$.

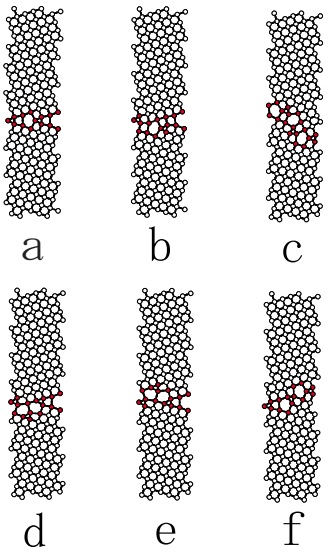

FIG. 5. (Color online) Atomic structures of $\Sigma=5$ Si[001](120) GB with rotation angle $\theta=36.87°$.

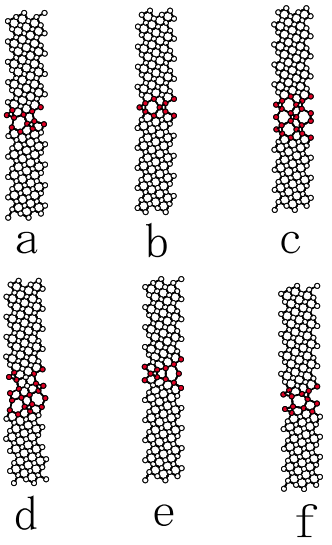

FIG. 6. (Color online) Atomic structures of $\Sigma=5$ Si[001](130) GB with rotation angle $\theta=53.15°$.

the multiplicity of GB structures in a given rotation angle. This multiplicity, which demonstrates the complexity of GB material, is also found in experiments.[19,20]

It is not surprising that the small angle GB will have lots of units of perfect-crystal lattice as the small angle will likely to add a small perturbation to the perfect crystal-like structure and introduce some dislocation cores.[9] The majority of the crystal-like units would like to be preserved. However, when the rotation angle becomes bigger, the number of crystal units will shrink and more dislocation core structures will be introduced. In Fig. 5 the rotation angle is increased to 36.87°. Structure Fig. 5(a) has a structure unit arrangement as *ACAC* in one period, which has two unit A dislocation cores separated by a single-crystal unit C, the burgers vector for the dislocations is the same as Fig. 5(a) structure while the number of C units are greatly decreased due to the larger orientation angle. Meanwhile the periodicity in the grain-boundary plane becomes much shorter compared to the low-angle grain-boundary structures in Fig. 4. In Fig. 5 other structures all have more complicated arrangement of dislocations cores and forms zigzag boundaries. Only structure Fig. 4(a) has a straight boundary plane and its energy is the lowest.

In Fig. 6 when the rotation angle is further increased to 53.15°, (130) boundary is formed and the period in the boundary plane is even shorter. Structure Fig. 6(b) has two dislocation core units A connected together and crystal unit is absent, making the structure units arrangement as simply *AA*. What is interesting is that in this case it is not the lowest-energy structures compared to the Fig. 6(a) structure, which is a zigzag structure of two A units. We can find that other metastable structures Figs. 6(c)–6(f) have more complicated dislocations connected together and structure Fig. 6(e) cannot be described by the three basic structural units A, B, and C defined above as the triangular and pentagonal rings are separated by a crystal unit. This might suggest that when the rotation angle becomes big, the matching of the two grains becomes flexible compared to the low-angle case and more exotic structures may appear, which is further illustrated in Fig. 7.

In Fig. 7 the rotation angle is 67.38°, making the GB a high-angle one. Structures in this rotation angle have been studied extensively both experimentally and theoretically in the previous work.[12,20,21] A variety of structures exist in this angle and interestingly, the structure with the lowest energy is the one that has the most dislocation dipole content.[12] Here using GA we have successfully reproduced all the structures reported in the literature and we also get some new structures constructing with different units. The structures in Fig. 7 are named according to the literature.[12] From the structural-unit viewpoint, most of the (150) structures can be constructed using a mixed dislocation core, B with crystal units C. For example, Fig. 7 (*S*20) and Fig. 7 (*S*11) have straight arrangement *BBCC* and *BCBC*, respectively, while Fig. 7 (*Z*20) and Fig. 7 (*Z*11) have zigzag arrangement *BBCC* and *BCBC*, respectively. There are also exceptions which the atomic

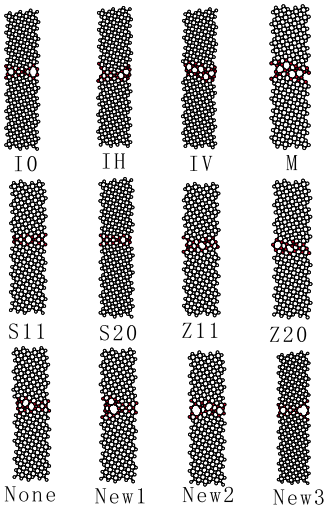

FIG. 7. (Color online) Atomic structures of $\Sigma=13$ Si[001](150) GB with rotation angle $\theta=67.38°$.

structures cannot be explained by the basic units arrangement. Figure 7 (*I*0), Fig. 7 (New1) and Fig. 7 (New2) all have very rare six member rings that are not found in GBs of other rotation angles. Figure 7 (New3) are similar to the Fig. 7 (*I*0) but with a larger outward shift between the two grains, which makes an eight member ring structure from the six ring structure. The multiplicity of these structures might be attributed to the fact that high-angle grain boundary gives more flexibility for atoms reconstructing in the GB area. Overall this high-angle grain boundary (150) has more dislocation cores than the low-angle ones. These structures have similar energies and that may be the reason why multiple structures can be observed in this angle experimentally with HRTEM and Z-contrast electron technique.[21]

IV. GRAIN-BOUNDARY-ENERGY CALCULATIONS

The structures obtained from the GA search are then used as starting points for first-principles and tight-binding calculations of the GB energies. This is done in the following way: a fully periodic system can be made by matching the two identical boundaries in the z direction together so that it will have periodicity in direction perpendicular to the boundary plane in addition to the periodicity in the x-y plane from the GA-generated structure. This method is similar to the one used in Ref. 12. In the new structure the two grain boundaries, which have opposite directions, are approximately 50 A apart, depending upon the details of the structures. The number of atoms range from 200 to over 1000 for all the structures we constructed. In these calculations, the dimension normal to the grain boundary is roughly ten times larger than the dimension along the boundaries, which are similar to the surface slab calculations. A set of four special k points is chosen to sample the two-dimensional rectangular Brillouin zone. All the atoms in the system are allowed to relax until the forces are less than 10 meV/A. The first-principles calculations are performed using the VASP code and tight-binding calculations are performed using the environment-dependent Si tight-binding potential developed by Wang and co-workers.[22] The grain-boundary energy is defined as

$$E_{\mathrm{GB}} = \frac{(E_{slab} - NE_{bulk})}{S_{\mathrm{GB}}}, \tag{1}$$

where N is the number of atoms in the structure, E_{bulk} is the bulk energy of silicon and S_{GB} is grain-boundary area.

Since first-principles calculations require lots of computational resources for large systems, a number of selected systems with shorter periods along the grain boundaries (Si[001](120) and Si[001](130)) are computed using *ab initio* techniques here. These are also the relatively high-angle grain-boundary structures that can exhibit multiple structures with similar energy. We also used environment-dependent tight-binding potential model for Si to test how well it produced the grain-boundary energy.[22] This potential goes beyond the two-center approximation by allowing the hopping terms to be modified by local atomic environment, which yields an improved transferability away from the bulk environment.

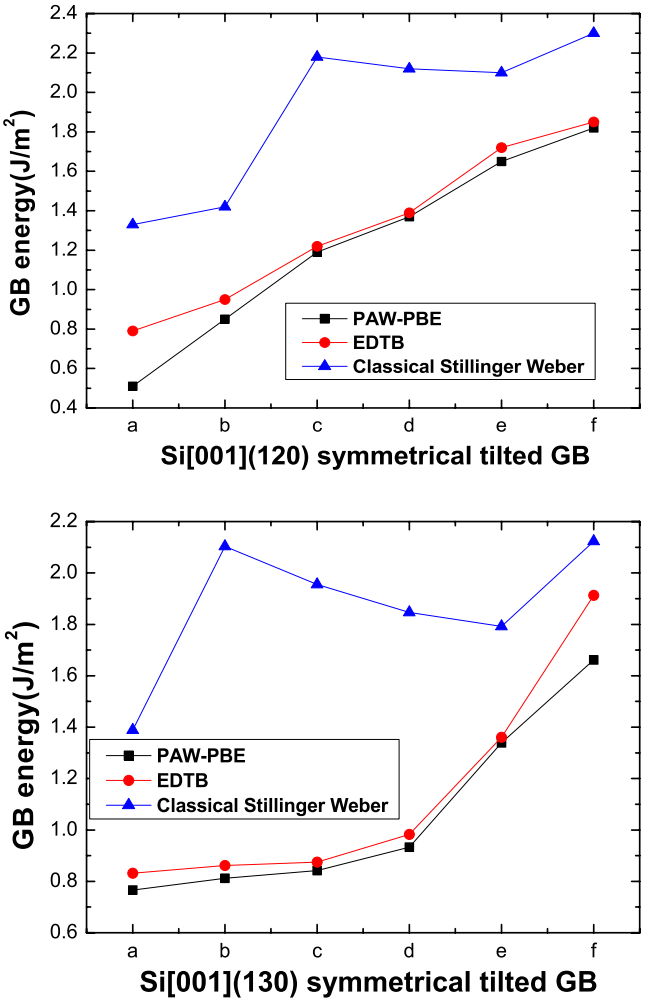

FIG. 8. (Color online) GB energies for Si[001](120) and Si[001](130) calculated in three different ways: DFT calculation, environmental-dependent tight-binding potential calculation, and classical Stillinger-Weber potential calculation.

In Fig. 8 we show the GB energies of several Si[001](120) and Si[001](130) structures. Those energy values are obtained from *ab initio* calculations, environment-dependent tight-binding potential and classical Stillinger-Weber potential. One striking observation is that result using tight-binding potential agrees very well with the first-principles calculation result while the classical potential gives a significant deviation. In particular, the tight-binding result gives the correct energy ordering and reasonably good energy difference in the structures while the classical potential cannot. This suggests that the classical potential, which performs fast in calculation, is good to be used in the genetic algorithm search to explore all the possible structures with high efficiency. However, the TB model can be effectively used as a calculation tool for examining these grain-boundary energies even with large unit cells. It has also been shown previously that the environment-dependent Si tight-binding potential also gives a good description of the energies Si[100](150) grain boundary.[12] Since the *ab initio* calculation requires a lot of computer time and resources, the TB potential model for Si can be used as a more suitable way

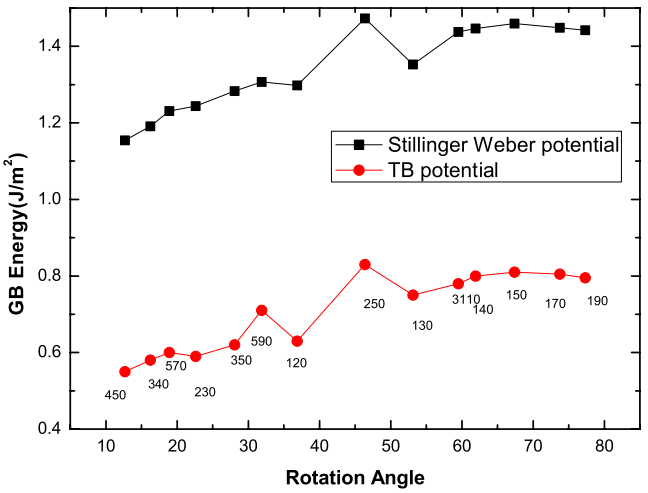

FIG. 9. (Color online) GB energies shown as a function of rotation angles.

to identify structures and calculating energies.

In Fig. 9 we show the lowest energies of GB in a given angle as a function of the total angles from both classical potential and tight-binding calculations. It can be seen that some lower period structures such as Si[100](120) and Si[100](130) have energies as the local minimums among the surrounding structures. Thus these structures, which have special angles and low periodicity, usually have the higher possibility of being observed in the experiment. In fact, faceting of the grain boundary can usually happen when the rotation angle of the GB is close to these special angles. Then faceting provides an efficient way of greatly reducing the GB energies.

V. SUMMARY

We developed a genetic algorithm to predict Si[001] symmetrical tilted grain boundary. This method is highly efficient and accurate for the grain-boundary-structure generation and reproduces all the structures both observed in experiments and deduced by the theoretical calculations. Almost all the GB structures can be expressed in the structural unit model except for a few high-angle cases in which six and eight ring structures appear. Starting from the low-angle grain boundary, as the disorientation angle between the grains becomes bigger, the number of perfect-crystal unit in the grain-boundary area will decrease and the connection between dislocation cores will become complex. The environment-dependent tight-binding potential for Si is used to evaluate the energy of selected grain-boundary structures and have a very good agreement with the first-principles calculation results. It provides us a useful tool for evaluating the energy orders of the structures and making corrections for the traditional classical potential results.

Besides the symmetrical tilted GB, more types of GBs including the twisted and asymmetrical ones can also be explored by the genetic algorithm in the similar way. This would be done in the later work. For Si GBs the environment-dependent tight-binding potential would always be a valuable tool for the GB energy calculation due to its high transferability.

ACKNOWLEDGMENTS

Ames Laboratory is operated for the U.S. Department of Energy by Iowa State University under Contract No. DE-AC02-07CH11358. This work was supported by the Director for Energy Research, Office of Basic Energy Sciences, including a grant of computer time at the National Energy Research Supercomputing Center (NERSC) in Berkeley. We are grateful to F. C. Chuang for his help in the development and understanding of the genetic algorithm. Min Ji is thanked for the discussion on the grain-boundary structures.

[1] R. Hornstra, Physica (Utrecht) **25**, 409 (1959).
[2] R. M. Grovenor, J. Phys. C **18**, 4079 (1985).
[3] T. A. Arias and J. D. Joannopoulos, Phys. Rev. B **49**, 4525 (1994).
[4] A. Maiti, M. F. Chisholm, S. J. Pennycook, and S. T. Pantelides, Phys. Rev. Lett. **77**, 1306 (1996).
[5] M. Kohyama, Phys. Status Solidi B **141**, 71 (1987).
[6] M. Kohyama, R. Yamamoto, Y. Ebata, and M. Kinoshita, J. Phys. C **21**, 3205 (1988).
[7] M. Kohyama, R. Yamamoto, and M. Doyama, Phys. Status Solidi B **137**, 11 (1986).
[8] T. Paxton and A. P. Sutton, J. Phys. C **21**, L481 (1988).
[9] A. Levi, D. A. Smith, and J. T. Weizel, J. Appl. Phys. **69**, 2048 (1991).
[10] A. P. Sutton and V. Vitek, Philos. Trans. R. Soc. London, Ser. A **309**, 1 (1983).
[11] O. A. Shenderova, D. W. Brenner, and L. H. Yang, Phys. Rev. B **60**, 7043 (1999).
[12] J. R. Morris, Z. Y. Lu, D. M. Ring, J. B. Xiang, K. M. Ho, C. Z. Wang, and C. L. Fu, Phys. Rev. B **58**, 11241 (1998).
[13] D. M. Deaven and K. M. Ho, Phys. Rev. Lett. **75**, 288 (1995).
[14] A. R. Oganov and C. W. Glass, J. Chem. Phys. **124**, 244704 (2006).
[15] F. C. Chuang, C. Z. Wang, and K. H. Ho, Phys. Rev. B **73**, 125431 (2006).
[16] F. C. Chuang, C. V. Ciobanu, V. B. Shenoy, C. Z. Wang, and K. M. Ho, Surf. Sci. **573**, L375 (2004).
[17] F. C. Chuang, C. V. Ciobanu, C. Predescu, C. Z. Wang, and K. M. Ho, Surf. Sci. **578**, 183 (2005).
[18] T. L. Chan, C. V. Ciobanu, F. C. Chaung, N. Lu, C. Z. Wang, and K. M. Ho, Nano Lett. **6**, 277 (2006).
[19] J. L. Rouviere and A. Bourret, in *Polycrystalline Semiconductors*, edited by H. J. Möller, H. P. Strunk, and J. H. Werner, Springer Proceedings in Physics Vol. 35 (Springer-Verlag, Berlin, 1989), p. 19.
[20] J. L. Rouviere and A. Bourret, J. Phys. (Paris) **51**, Cl-329 (1990).
[21] M. F. Chisholm and S. J. Pennycook, MRS Bull. **22**, 53 (1997).
[22] M. S. Tang, C. Z. Wang, C. T. Chan, and K. M. Ho, Phys. Rev. B **53**, 979 (1996).